Journal of Magnetic Resonance **139,** 18–25 (1999)
Article ID jmre.1999.1767, available online at http://www.idealibrary.com on IDEAL®

Transforming NMR Data Despite Missing Points

Dean O. Kuethe,*[,1] Arvind Caprihan,† Irving J. Lowe,‡ David P. Madio,‡[,2] and H. Michael Gach‡[,3]

**Lovelace Respiratory Research Institute, †New Mexico Resonance, 2425 Ridgecrest Drive SE, Albuquerque, New Mexico 87108; and ‡Department of Physics and Astronomy, University of Pittsburgh, and Pittsburgh NMR Center for Biomedical Research, Mellon Institute, 4400 Fifth Avenue, Pittsburgh, Pennsylvania 15213*

Received November 3, 1998; revised March 25, 1999

Some NMR experiments produce data with several of the initial points missing. The inverse discrete Fourier transform (IDFT) assumes these points are present so the data cannot be so transformed without artifact-ridden results. This problem is often particularly severe when projection imaging with free-induction decays (FIDs). This paper compares recent methods for obtaining a projection from incomplete data and elaborates on their strengths and limitations. One method is to write the transform that would take the desired projection to the truncated data set, and then solve the matrix equation by singular value decomposition. A second replaces the missing data with zeros, so that an IDFT produces a projection with unwanted artifacts. Then one solves the matrix equation that takes the desired projection to the artifact-ridden projection. A third uses the same artifact-ridden projection, but fits the region outside the bandwidth of the sample with as many sinusoidal functions as there are missing data. The coefficients of these functions are estimates of the missing data, and the projection is obtained by transforming the completed FID or subtracting the extrapolation of the fitted curve from the region containing the object. We show that when all three methods are applicable, they theoretically produce the same result. They differ by ease of implementation and possibly by computational errors. They give a result similar to that of the previous method that iteratively corrects the FID and projection after repeated IDFTs and DFTs. We find that one can obtain a projection despite missing a substantial number of data.

Key Words: **partial-data transform; compact support; band-limited; extrapolation; Gerchberg–Papoulis.**

INTRODUCTION

In projection imaging with free-induction decays (FIDs), the initial part of the signal cannot be sampled during radio transmission, or during recovery of the receiver and associated filters. One is faced with the problem of constructing a projection (1D image) without the initial data. Usually, in NMR spectroscopy, only a few data are missing and the spectrum is corrected by adjusting the baseline and phase. When more spectroscopy data are missing, they can be extrapolated after fitting the FID with a series of damped complex exponentials (*1*), or the artifact produced in the spectrum can be approximated and subtracted (*2*). In solid state NMR with short T_2 samples, the problem is more serious and the solutions are more specialized (*3*). In our applications of imaging with FIDs the problem is severe and the corrections used in spectroscopy do not result in a satisfactory projection. The applied magnetic field gradient makes the FID decay fast, and implies many frequency components, making a curve fit more difficult. It is helpful to oversample the data, i.e., collect data at a frequency greater than that of the bandwidth of the object. Then the object occupies a limited region of the projection, and one can use the knowledge that the projection should be zero outside that region. Gerchberg (*4*) and Papoulis (*5*) used this fact in their iterative technique. An inverse discrete Fourier transform (IDFT) of the known portion of the signal, along with zeros substituted for missing data, yields a projection that is then set to zero outside the bounds of the object. Then a DFT yields a FID, which in turn is modified by replacing the known segment with the original data. This procedure is iterated until it converges to yield an estimate for the missing data points and the projection.

Jain and Ranganath (*6*) presented a generalization of transforming partial data from band-limited signals, which Plevritis and Macovski (*7*) applied to NMR imaging to construct images of spatially bounded objects despite the fact that data were missing from the ends of echoes. Both references express the problem as an ill-conditioned matrix equation, which is improved using known constraints of the object, and suggest solving it by singular value decomposition (SVD). An extensive review of transforming partial data sets for NMR imaging appears in Liang *et al.* (*8*). McGibney *et al.* (*9*) compare some of these methods and evaluate their usefulness in NMR imaging. The development of the non-iterative techniques was not directed toward the problem of data missing from the beginnings of FIDs (the center of "*k*-space" in imaging jargon). The Gerchberg–Papoulis algorithm remained the method of choice

[1] To whom correspondence should be addressed: LRRI, 2425 Ridgecrest Drive SE, Albuquerque, NM 87108. Fax: (505) 262-7043, E-mail: dkuethe@LRRI.org.

[2] Current address: Schlumberger-Doll Research, Old Quarry Road, Ridgefield, CT 06877.

[3] Current address: GE Medical Systems, P.O. Box 414, W832, Milwaukee, WI 53201.

1090-7807/99 $30.00

for this problem. We recently proposed two more non-iterative methods (*10, 11*) to address these early missing data. Plevritis and Macovski's (*7*) method can also be applied to early missing data, so three non-iterative methods are available to solve the same problem. In this paper, we demonstrate that when all three methods are applicable, they will theoretically yield the same result because they imply that the same matrix equation is satisfied. In addition, when the Gerchberg–Papoulis algorithm converges, it should also yield the same result. The calculations are different, however, so the methods may differ by errors in computation. One method is easy to program to include non-integral numbers of missing data and situations when the data are not oversampled. We discuss it in detail to show the limitations of these methods.

DEFINITION OF THE PROBLEM

We seek a one-dimensional (1D) discrete image, or projection, $\mathbf{x} = \text{col}(x_0, x_1, \ldots, x_{N-1})$. The digitized signal with no missing points will be represented by $\mathbf{s} = \text{col}(s_0, s_1, \ldots, s_{N-1})$, where $s_0, s_1, \ldots, s_{(N/2)-1}$ is one FID with a positive magnetic field gradient and $s_N, s_{N-1}, \ldots, s_{N/2}$ is another FID with a negative one. Because $s_N = s_0$, it may be excluded from **s**. The relationship between **s** and **x** is given by the DFT,

$$s_n = \sum_{m=0}^{N-1} x_m e^{-i\frac{2\pi}{N}mn}, \quad \text{for } n = 0, 1, \ldots, N-1. \quad [1]$$

In matrix form

$$\mathbf{s} = \mathbf{F}\mathbf{x}, \quad [2]$$

where $F_{mn} = e^{-i(2\pi/N)mn}$. **x** is the IDFT of **s**, $\mathbf{x} = \mathbf{F}^{-1}\mathbf{s}$, where $F^{-1}_{mn} = \frac{1}{N}e^{i(2\pi/N)mn}$. DFT properties imply that the signal **s** and the projection **x** can be extended periodically; i.e., for all n, $x_n = x_{N+n}$ and $s_n = s_{N+n}$. We may write

$$s_n = \sum_{m=-\frac{N}{2}}^{\frac{N}{2}-1} x_m e^{-i\frac{2\pi}{N}mn}, \quad \text{for } n = 0, 1, \ldots, N-1. \quad [3]$$

By tolerating negative indices for the elements of **x**, the zero frequency coefficient is in the center of the vector, where we are used to seeing the center of an object.

The signal **s** is obtained by sampling a continuous signal at interval Δt, which implies that the bandwidth F_b of **x** is $1/\Delta t$, and the elements of **x** are frequency coefficients separated by $\Delta f = F_b/N$. The discrete image is related to the object by the point–spread function (*12*). For a dead time T_d, the interval between the center of the radio pulse and the first datum, the number of points missing from each FID is

$$q = \frac{T_d}{\Delta t}. \quad [4]$$

T_d does not have to be an integer multiple of Δt so q can be non-integer, but for the purposes of comparing methods we consider q to be integer. Our task is to find **x**, even when elements $s_0, s_1, \ldots, s_{q-1}$ and $s_N, s_{N-1}, \ldots, s_{N-q+1}$ are missing. The total number of points missing from **s** is $2q - 1$, because the first point $s_0 = s_N$ is common to each FID.

COMMON NOTATION FOR THREE METHODS

Method 1

To develop a matrix formulation common to the three methods, we represent the completeness of the data by an $N \times N$ diagonal matrix **C**, where $C_{nn} = 1$, if the nth data point is present, and $C_{nn} = 0$, if the nth data point is missing. Then

$$\mathbf{d} = \mathbf{C}\mathbf{s} \quad [5]$$

defines the data set with zeros substituted for the missing points.

Similarly, the knowledge that some of the elements **x** are zero is represented by

$$\mathbf{x} = \mathbf{T}\mathbf{x}, \quad [6]$$

where **T** is an $N \times N$ diagonal matrix, with $T_{nn} = 1$, if $x_n \neq 0$, and $T_{nn} = 0$ otherwise. Thus, Eq. [2] with truncated data and band-limited projection is

$$\mathbf{d} = \mathbf{C}\mathbf{F}\mathbf{T}\mathbf{x}. \quad [7]$$

Trying to solve this equation represents the method of Kuethe *et al.* (*10*). To see the relationship to their formula, consider in Eq. [3] that $x_n \neq 0$, for $n = -M/2, \ldots, 0, \ldots, (M/2) - 1$, where $M \leq N$, and zero otherwise. It then becomes

$$d_n = \sum_{m=-\frac{M}{2}}^{\frac{M}{2}-1} x_m e^{-i\frac{2\pi}{N}mn}, \quad \text{for } n = q, \ldots, N-q. \quad [8]$$

Assuming Eq. [7] is indexed like Eq. [1] this is equivalent to defining $C_{nn} = 1$, for $n = q, q+1, \ldots, N-q$, and zero otherwise and $T_{nn} = 1$, for $n = 0, 1, \ldots, (M/2) - 1$ and $n = N-1, N-2, \ldots, N-(M/2)$, and zero otherwise. Equation [8] contains only the non-zero terms of Eq. [7]. If $M < N$, the object bandwidth $F_o = M\Delta f$ is less than the data sampling bandwidth $F_b = 1/\Delta t$, and the data are said to be "oversampled" because $\Delta t < 1/F_o$. To make computer programming easier we rearrange the indices of Eq. [8] to run

from 0 to N_c, the number of data collected, $N_c = N - 2q + 1$, in the data vector $\bar{\mathbf{d}}$ with $\bar{d}_n = d_{n+q}$, and to run from 0 to $M - 1$ in $\bar{\mathbf{x}}$, with $\bar{x}_m = x_{m-(M/2)}$; then

$$\bar{d}_n = \sum_{m=0}^{M-1} \bar{x}_m e^{-i\frac{2\pi}{N_c+2q-1}(m-\frac{M}{2})(n+q)}, \quad \text{for } n = 0, 1, \ldots, N_c - 1, \quad [9]$$

is the formula of Kuethe *et al.* (*10*), with the object centered around $\bar{x}_{M/2}$. In matrix form,

$$\bar{\mathbf{d}} = \mathbf{A}\bar{\mathbf{x}}, \quad [10]$$

where

$$A_{mn} = e^{-i\frac{2\pi}{N_c+2q-1}(m-\frac{M}{2})(n+q)}.$$

$\mathbf{A}$ is an $(N - 2q + 1) \times M$ matrix. M need not be less than N. When q is non-integer, $N_c = N - 2q + 1$ is integer but $N = N_c + 2q - 1$ is not.

The SVD of $\mathbf{CFT}$ or $\mathbf{A}$ provides a pseudo inverse by minimizing $\|\mathbf{d} - \mathbf{CFTx}\|$ or $\|\bar{\mathbf{d}} - \mathbf{A}\bar{\mathbf{x}}\|$, where for any vector $\mathbf{z}$, $\|\mathbf{z}\|^2 = \sum (\text{real}(z_k)^2 + \text{imaginary}(z_k)^2)$. Non-unique solutions are resolved by minimizing $\|\mathbf{x}\|^2$. In other words, we get a least-squares fit with the smallest-possible frequency coefficients. Most pre-programmed SVD routines (e.g., *13*), do not accept complex matrices, a limitation overcome by writing the complex matrix equation $(\mathbf{A}_R + i\mathbf{A}_I)(\mathbf{x}_R + i\mathbf{x}_I) = \mathbf{d}_R + i\mathbf{d}_I$ as a real equation

$$\begin{vmatrix} \mathbf{A}_R & -\mathbf{A}_I \\ \mathbf{A}_I & \mathbf{A}_R \end{vmatrix} \begin{vmatrix} \mathbf{x}_R \\ \mathbf{x}_I \end{vmatrix} = \begin{vmatrix} \mathbf{d}_R \\ \mathbf{d}_I \end{vmatrix}.$$

Method 2

In the method of Madio, Gach, and Lowe (*11*) we attempt to find the missing points by analyzing the region of the artifact-ridden projection outside the object. It should be zero but is a sum of sinusoids and noise. The negatives of the missing data are the complex coefficients of the sinusoids, which can be estimated by a least-squares curve fit. Inserting the missing data, thus obtained, into the FID and performing an IDFT are equivalent to fitting the artifact outside the object to the sum of sinusoids and subtracting the curve, with its extrapolation into the region containing the object, from the entire projection. In this method, we calculate $2q - 1$ unknowns from $N - M$ knowns, while in the previous method we solved for M unknowns from $N - 2q + 1$ knowns. Let us decompose the signal $\mathbf{s}$ into two components $\mathbf{d}$ and $\mathbf{a}$, where $\mathbf{d}$, as defined before, contains the observed components of $\mathbf{s}$ and zeros substituted for missing point, and $\mathbf{a}$ consists of the missing part of $\mathbf{s}$,

$$\mathbf{s} = \mathbf{d} + \mathbf{a} = \mathbf{Cs} + \mathbf{C}^c\mathbf{s}, \quad [11]$$

where $\mathbf{C}^c = \mathbf{I} - \mathbf{C}$, and $\mathbf{I}$ is the identity matrix. The projection $\mathbf{x}$ is given by the inverse DFT of $\mathbf{s}$, in other words

$$\mathbf{x} = \mathbf{F}^{-1}\mathbf{s} = \mathbf{F}^{-1}\mathbf{d} + \mathbf{F}^{-1}\mathbf{a}. \quad [12]$$

We define

$$\mathbf{y} = \mathbf{F}^{-1}\mathbf{d}, \quad [13]$$

the artifact-ridden projection. If we multiply Eq. [12] by $\mathbf{T}^c = \mathbf{I} - \mathbf{T}$, we get

$$\mathbf{T}^c\mathbf{y} + \mathbf{T}^c\mathbf{F}^{-1}\mathbf{C}^c\mathbf{a} = 0, \quad [14]$$

where we have used the fact that $\mathbf{T}^c\mathbf{x} = 0$ and inserted $\mathbf{C}^c\mathbf{a} = \mathbf{a}$ to enforce the dimensions of the problem. We can solve for $\mathbf{a}$ by minimizing $\|\mathbf{T}^c\mathbf{y} + \mathbf{T}^c\mathbf{F}^{-1}\mathbf{C}^c\mathbf{a}\|$ and substituting it in Eq. [12] to obtain $\mathbf{x}$. Equation [14] has a number of unnecessary terms that we eliminate by writing Eq. [12] as

$$x_m = y_m + \frac{1}{N}\sum_{n=0}^{N-1} a_n e^{i\frac{2\pi}{N}mn}, \quad \text{for } m = 0, 1, \ldots, N - 1, \quad [15]$$

and eliminating all but zero terms of $\mathbf{x}$ and non-zero terms of $\mathbf{a}$. a_n are non-zero for n from 0 to $q - 1$ and from $N - q + 1$ to $N - 1$. Periodicity allows us to replace the $N - q + 1$ to $N - 1$ indices with $-q + 1$ to -1 and write

$$0 = y_m + \frac{1}{N}\sum_{n=-q+1}^{q-1} a_n e^{i\frac{2\pi}{N}mn}, \quad \text{for } m = \frac{M}{2}, \frac{M}{2} + 1, \ldots, N - \frac{M}{2} - 1. \quad [16]$$

By defining $\bar{\mathbf{y}}$ and $\bar{\mathbf{a}}$, with $\bar{y}_m = y_{m+(M/2)}$ and $\bar{a}_n = a_{n-(q-1)}$, we obtain a more convenient form

$$\bar{y}_m + \frac{1}{N}\sum_{n=0}^{2(q-1)} \bar{a}_n e^{i\frac{2\pi}{N}(m+\frac{M}{2})(n-q+1)} = 0, \quad \text{for } m = 0, 1, \ldots, N - M - 1. \quad [17]$$

In matrix form

$$\bar{\mathbf{y}} + \mathbf{B}\bar{\mathbf{a}} = 0, \quad [18]$$

where $\mathbf{B}$ is $(N - M) \times (2q - 1)$, with

$$B_{mn} = \frac{1}{N} e^{i\frac{2\pi}{N}(m+\frac{M}{2})(n-q+1)}.$$

The missing points can be found by minimizing either $\|\mathbf{T}^c\mathbf{y} + \mathbf{T}^c\mathbf{F}^{-1}\mathbf{C}^c\mathbf{a}\|$ or $\|\bar{\mathbf{y}} + \mathbf{B}\bar{\mathbf{a}}\|$ with the help of SVD.

Method 3

Kuethe *et al.*'s (*10*) method minimizes the size of a time-domain vector $\|\mathbf{d} - \mathbf{CFTx}\|$. Plevritis and Macovski's (*7*) method does a similar minimization in the frequency domain. Applying $\mathbf{F}^{-1}$ to Eq. [7] and using $\mathbf{y} = \mathbf{F}^{-1}\mathbf{d}$ (Eq. [13]) yields

$$\mathbf{y} = \mathbf{F}^{-1}\mathbf{CFTx}, \qquad [19]$$

which is solved for $\mathbf{x}$ by minimizing $\|\mathbf{y} - \mathbf{F}^{-1}\mathbf{CFTx}\|$.

EQUIVALENCE OF THE METHODS

The quantities to be minimized by Kuethe *et al.*'s method (*10*) and by Plevritis and Macovski's (*7*) method differ by an invertible (in fact, unitary within a constant) matrix $\mathbf{F}^{-1}$. Thus, the information content is identical and both methods give the same answer. To be explicit, the $\mathbf{x}$ that minimizes $\|\mathbf{d} - \mathbf{CFTx}\|$ must satisfy the equation

$$\mathbf{T}^*\mathbf{F}^*\mathbf{C}^*(\mathbf{d} - \mathbf{CFTx}) = 0, \qquad [20]$$

where for any complex matrix $\mathbf{A}$, $\mathbf{A}^*$ is the conjugate transpose of $\mathbf{A}$ (*14*). Similarly, the $\mathbf{x}$ that minimizes $\|\mathbf{y} - \mathbf{F}^{-1}\mathbf{CFTx}\|$ must satisfy

$$\mathbf{T}^*\mathbf{F}^*\mathbf{C}^*(\mathbf{F}^{-1})^*(\mathbf{y} - \mathbf{F}^{-1}\mathbf{CFTx}) = 0. \qquad [21]$$

Substituting $\mathbf{F}^{-1}\mathbf{d}$ for $\mathbf{y}$ and noting that $(\mathbf{F}^{-1})^* = (\mathbf{F}^*/N)^* = \mathbf{F}/N$, we find that Eq. [21] is identical to Eq. [20]; therefore, the two solutions are identical.

Next we show that Madio, Gach, and Lowe's (*11*) result satisfies the same equation. In their method, $\mathbf{a}$ is obtained by minimizing $\|\mathbf{T}^c\mathbf{y} + \mathbf{T}^c\mathbf{F}^{-1}\mathbf{C}^c\mathbf{a}\|$, so it must satisfy

$$\mathbf{C}^{c*}(\mathbf{F}^{-1})^*\mathbf{T}^{c*}(\mathbf{T}^c\mathbf{y} + \mathbf{T}^c\mathbf{F}^{-1}\mathbf{C}^c\mathbf{a}) = 0. \qquad [22]$$

Substituting $\mathbf{C}^c$ for $\mathbf{C}^{c*}$, $\mathbf{F}/N$ for $(\mathbf{F}^{-1})^*$, $\mathbf{T}^c$ for $\mathbf{T}^{c*}$, $\mathbf{F}^{-1}\mathbf{d}$ for $\mathbf{y}$, and $\mathbf{a}$ for $\mathbf{C}^c\mathbf{a}$ and noting that $\mathbf{T}^c\mathbf{T}^c = \mathbf{T}^c$ yield

$$\mathbf{C}^c\mathbf{F}\mathbf{T}^c\mathbf{F}^{-1}(\mathbf{d} + \mathbf{a}) = 0. \qquad [23]$$

Substituting $\mathbf{I} - \mathbf{T}$ for $\mathbf{T}^c$ and noting that $\mathbf{C}^c\mathbf{d} = 0$ before substituting $\mathbf{I} - \mathbf{C}$ for $\mathbf{C}^c$ yield

$$\mathbf{a} - \mathbf{FTF}^{-1}(\mathbf{d} + \mathbf{a}) + \mathbf{CFTF}^{-1}(\mathbf{d} + \mathbf{a}) = 0. \qquad [24]$$

Pre-multiplying by $\mathbf{TF}^{-1}$ and substituting x from Eq. [12] into the last term yield

$$\mathbf{TF}^{-1}\mathbf{a} - \mathbf{TF}^{-1}(\mathbf{d} + \mathbf{a}) + \mathbf{TF}^{-1}\mathbf{CFTx} = 0. \qquad [25]$$

By noting that $\mathbf{CC} = \mathbf{C}$ and $\mathbf{Cd} = \mathbf{d}$,

$$\mathbf{TF}^{-1}\mathbf{C}(\mathbf{d} - \mathbf{CFTx}) = 0. \qquad [26]$$

Because $\mathbf{F}^{-1} = \mathbf{F}^*/N$, $\mathbf{T}^* = \mathbf{T}$, and $\mathbf{C}^* = \mathbf{C}$, Eq. [26] is identical to Eq. [20]; therefore, the two solutions are identical.

The band-limiting constraint for the Gerchberg–Papoulis algorithm is the same as $M < N$ in the above three methods. Papoulis (*5*) proves that convergence implies the minimization of the same two quantities as SVD, so the Gerchberg–Papoulis algorithm also provides the same answer, a least-squares fit of the M frequency components to the N_c data, with the sum of squares of the frequency components also minimized. The matrix methods will generally be faster than iteration because once a pseudo inverse is calculated, it can be applied to multiple lines of data. The iteration must be repeated for each line of data.

Although the matrix methods involve different calculations to minimize different quantities, they should give the same answer. Two methods differ only by an invertible matrix and should have identical properties. The method of Madio, Gach, and Lowe (*11*) is different in implementation because the minimization is in a vector space complementary to that of the other two methods. It solves for $(2q - 1)$ unknowns from $(N - M)$ equations, while the others solve for M unknowns from $(N - 2q + 1)$ equations. It requires oversampling, while the others do not.

PRACTICAL CONSIDERATIONS

Oversampling and Condition Number

We will use the method of Kuethe *et al.* (*10*), which solves Eq. [9] for $\bar{\mathbf{x}}$ by singular value decomposition of $\mathbf{A}$ in Eq. [10] to illustrate some of the limitations of these methods. It does not require oversampling ($N > M$) so we can see the problems that arise when the number of data is smaller than the number of points we seek in the projection ($N_c < M \leq N$). If we try to find all $M = N$ frequency coefficients that make up the projection $\mathbf{x}$, we are fitting the data with a full range of sinusoids. By including the highest frequency components, we can fit "discontinuities" in the periodically extended discrete signal. Even if the known part of the signal is smooth, a DFT of the $\mathbf{x}$ we obtain may jump from one point to the next in the region over which we are missing data. Consider $q = 1$, so we are missing s_o and $N_c = N - 1$. If $M = N$, the $\mathbf{x}$ we obtain may imply any s_o. If $\mathbf{x}$ has a zero baseline in its high frequen-

cies, it implies an s_o similar to its neighbors s_1 and s_{N-1}. A baseline offset implies that s_o is dissimilar from its neighbors. The projection we obtain with $q = 1$ and $M = N$ will have the baseline offset that minimizes $\|\bar{\mathbf{x}}\|$, even if the true projection has a zero baseline. Lowering M by one, to N_c, restores the baseline. The artifacts we obtain with $M = N$ and $q = 1, 2, 3$, etc., are similar to the artifacts that Madio, Gach, and Lowe (*11*) describe in the artifact-ridden projection as successive points of data are replaced by zeros. The difference is that the missing points are set to whatever value minimizes $\|\bar{\mathbf{x}}\|$ instead of zero. In conclusion, we must at least oversample so that $M \leq N_c$ to obtain artifact-free results.

One of our pleasant surprises is that one can miss a substantial portion of data and still obtain a satisfactory projection. As an index of success at solving for $\bar{\mathbf{x}}$, it is useful to compute the condition number C_N (the ratio of the largest to the smallest singular value of **A**). For an invertible matrix, such as the DFT, $C_N = 1$. The larger the C_N, the more underdetermined the problem, and the better quality data one needs to obtain meaningful results. As a crude guide, $C_N < 20$ is good, $C_N > 10^4$ is bad. In practice, the methods fail in one of two ways. Either the numerical routine for finding the decomposition fails to converge, or the data are too inaccurate or noisy. Failure to converge is either a result of computing with insufficient precision or asking for too much, i.e., asking for a reasonable guess for solutions to an inferior class of matrix equations. (In addition, large matrices may require more iteration than preprogrammed routines allow.) In our experience, failure to converge in double precision means that the condition number is so large ($>10^{10}$) that even if one could compute the pseudo inverse using greater precision, it would be of no practical use because no NMR data are precise enough. When the SVD algorithm converges but the data are poor, the resulting frequency coefficients are unreasonably large compared to those one would expect. There are many sets of unreasonably large frequency components that may produce a slightly better fit than the correct set, and without sufficient data, the correct set is an unlikely guess.

To improve C_N, increase N by oversampling, and make M as small as possible by solving for only those frequency coefficients known to be non-zero (i.e., do not try to compute extra coefficients, outside the object). Of course, lowering q lowers C_N. For a given M, oversampling increases N and q by the same factor and may raise C_N slightly, but nonetheless the result improves. Increasing N, M, and q, all by the same factor, raises C_N, but does not degrade the result unless C_N is so high that it is bordering the precision of computation. Even though the Madio, Gach, and Lowe (*11*) method produces a matrix different from that of the Kuethe *et al.* (*10*) method, C_N is the same. In most cases one would choose the method that produces the smaller matrix. It is faster to find the SVD of the smaller matrix. We find that in practice, they do indeed produce the same result, so long as the problem is not bordering the precision of computation.

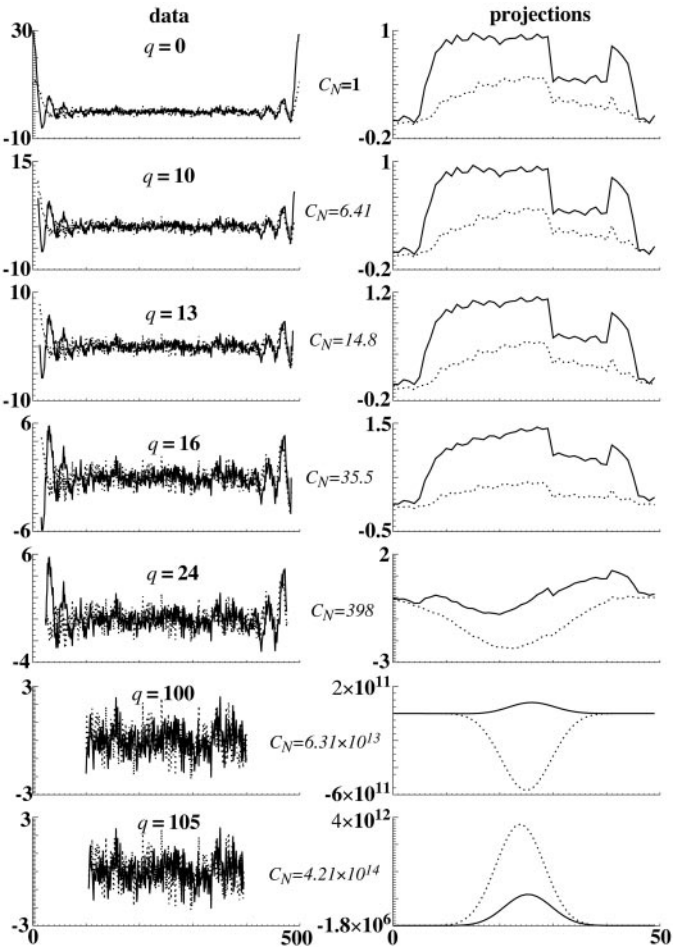

FIG. 1. The left column of graphs shows a set of synthetic data **s**. It is the sum of the DFT of a projection **x** (see Fig. 2) and simulated Gaussian noise. Solid lines are real parts; dashed lines are imaginary. The noise has a standard deviation that is 1/30 the magnitude of s_o, so the signal-to-noise ratio (SNR) of the FIDs is 30. The q value on each graph is the number of points missing from each FID; the vertical scale of the graphs decreases as the larger data are removed to show more clearly the remaining data. The projections obtained from these data are shown in the graphs to the right. Their vertical scales vary by 12 orders of magnitude. For each pair of graphs, C_N is the condition number of the matrix that takes a projection with $M = 50$, to a data set with $N_c = N - 2q + 1$, with $N = 500$. $N/M = 10$. The projections change imperceptibly as q varies from 0 to 10. The projection is distorted when C_N is approximately the SNR. As C_N increases further, the ability to obtain the projection is lost, and the size of the projection becomes huge.

An unexpected result is that as one removes points from a data set, the projections are virtually identical (graph one on top of the other) until the method fails from insufficient data (Fig. 1). As a crude guide, one can miss the number of points that correspond to one cycle of the highest frequency component before the method fails (i.e., $q < N/M$). As a less crude guide, one is safe if the signal-to-noise ratio of the data is greater than C_N (Figs. 1 and 2). With highly precise and accurate data, one can miss a great many points and still obtain the projection (Fig. 2). An instructive example of the limit is

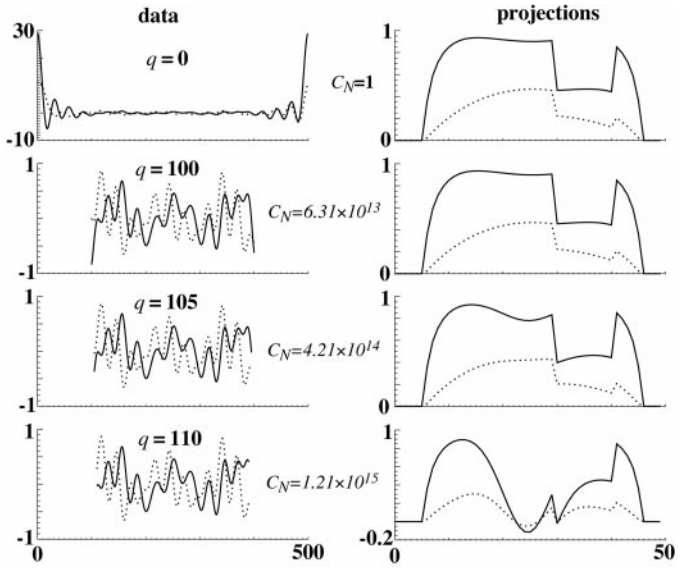

FIG. 2. The data in the top left graph are a double-precision DFT of the projection in the top right graph (zero-filled to 500 points), so the signal-to-noise ratio is approximately 10^{14}. These data are the same as those in Fig. 1, without the added synthetic noise. With these more precise data, q can be much larger, i.e., 100 as opposed to 13, and one can still obtain the projection. As in Fig. 1, when the condition number becomes as large as the SNR, the projection becomes distorted.

trying to calculate a projection, complete with phase information, from a single FID, i.e., $N_c = N/2 - q$, by solving

$$\bar{d}_n = \sum_{m=0}^{M-1} \bar{x}_m e^{-i\frac{\pi}{N_c+q}\left(m-\frac{M}{2}\right)(n+q)},$$

$$\text{for } n = 0, 1, \ldots, N_c - 1. \quad [27]$$

If $M = N_c$, even if $q = 0$, the matrix is singular (the determinant is zero) and we cannot solve the equation meaningfully. We can obtain a SVD of this matrix if $M < N_c$; however, the condition number is so large that artificial data calculated with double precision will yield a projection but single-precision data will not. An alternative way to obtain a projection with one FID is to ensure that the phase at time zero is zero and then construct the other half of the data as the complex conjugate of the existing data, which is the same as assuming that all the initial phases are zero. Although one cannot obtain phase information in this way, it reduces the amount of information being sought by half and, if the assumption holds, results in a good projection.

Typically, one realizes the full power of SVD when C_N is large by setting the most extreme singular values to zero before computing the pseudo inverse. We find that when C_N is large enough or the data noisy enough that the projection, computed using all singular values, becomes a very large smooth hump, this practice will return the projection to a reasonable size and may recover some recognizable features, but it will not result in a good projection. When C_N and noise are in the range where the projection is recognizable, altering the singular values will destroy it. This is even true for the high C_N examples shown in Fig. 2.

Spectroscopy Data Present a Challenge for These Methods

For most spectroscopy data, the periodic extension is discontinuous; i.e., the signal decays smoothly from s_0 to s_{N-1},

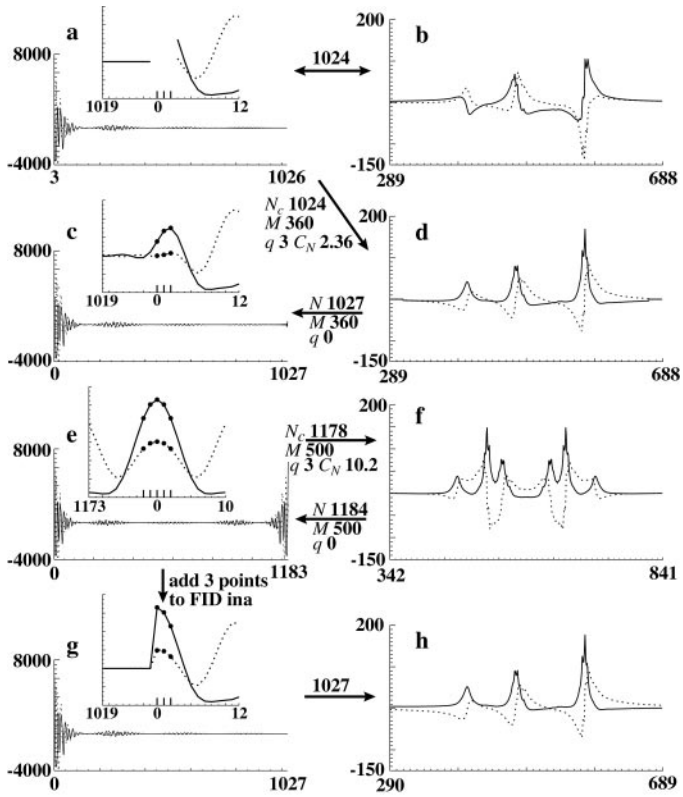

FIG. 3. (a) A 1024 point FID and (b) its IDFT. The inset in (a) displays the break in the periodic data that results from missing the first three points. Typically, spectra like (b) need phase adjustments because of these missing points. (d) The result of transforming (a) with the pseudo inverse of the matrix that takes the 360 points containing the peaks of the spectrum to the 1024 points of a full 1027 point data set, missing its first three points. The baseline is too good; i.e., it decays to zero faster than the tails of Lorentzian peaks. If we DFT (d) to obtain a FID (c), we find that the guesses for the missing points construct a smooth curve for the periodic data, rather than the jump expected for spectroscopy data. To obtain a better estimate of the missing points, we take the first 589 points of the FID in (a) (it is not necessary to use all 1024) and reflect them to obtain a 1178 point data set whose periodic extension would be continuous if it contained the missing points. We compute 500 of the frequency coefficients (f) (a superposition of two reflected spectra) with these data, and use (f) to compute the missing points (three on each end of the double FID data set). The inset of (e) shows that the newly computed missing points again form a continuous curve, but are better guesses than those in (c). (g) A complete FID (the three newly computed points added to (a) and its inverse DFT (h) is a more typical looking spectrum than (d) that needs less phase correction than (b).

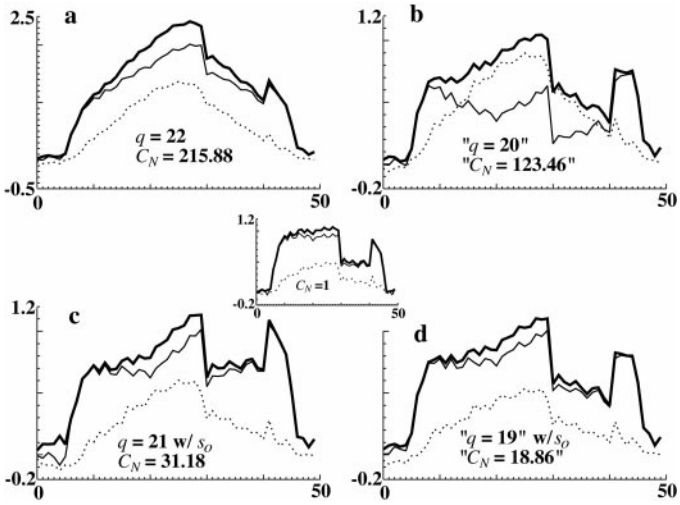

FIG. 4. (a) A projection obtained from the data in Fig. 1 with 22 points missing from either end. The condition number C_N of the decomposed matrix is high and the projection is too large, and distorted into too smooth a hump. The bold curve is the magnitude of the projection; solid and dashed curves are real and imaginary, respectively. The inset between the four graphs shows the true projection. (b) A projection obtained from the same data as (a) but using the pseudo inverse of a lower C_N matrix that assumes there are only 20 data missing from each end of a 496 point data set. Compared to (a), it appears edge-enhanced. It is fortuitously the correct size, but the phase is distorted. Projections (c) and (d) are the correct size with reason. They were obtained after addition of s_o to either end of the data set. C_N's are substantially lower. Projection (c) uses the correct number of missing data; projection (d), like (b), fibs by two. Even though C_N's for (c) and (d) are reasonably low, the projections are not as good as those for similar C_N's in Fig. 1 because many of the least noisy data are missing.

then jumps to $s_N = s_o$. In contrast to the example in Eq. [27], one FID is considered to be a complete set of data, instead of half a set of data. (The fictitious analog to "the other FID" in imaging data would result if one could reverse the relative spin frequencies—higher to lower and *vice versa.*) The DFT models the signal as the discrete sum of *non-decaying* sinusoids. The only way to construct the discontinuity in spectroscopy data is for all frequency components (notably the highest frequency ones) to be non-zero. Thus, spectroscopy data cannot be band-limited in the same sense as imaging data. A related difference between spectroscopy and imaging is that the phase of a spectrum is not uniform, even when the radio transmission successfully starts all the spins at the same phase. The frequency components have the initial phases necessary to construct the discontinuity. In imaging, the phase can be uniform.

It is tempting to use these methods for spectroscopy by treating one FID as a full data set missing only a few points at the beginning (i.e., put a 2 in front of the π in Eq. [27]) with the expectation that the phase will be similar to a typical spectrum but require less correction. However, the result is a baseline that decays uncharacteristically to zero at the high frequency ends, and the guesses for the missing points create a smooth curve between s_{N-1} and s_o (Fig. 3). To obtain points missing from spectroscopy data, construct another half of a bigger data set as the mirror of the first (not the conjugate of the mirror, because that makes the unlikely assumption that the phase of s_o is zero), then treat it like the double FID imaging data. The spectrum will be a confusing superposition of two mirror spectra, but the guesses for the missing points will be reasonable.

A Couple More Tricks to Reduce the Condition Number

When imaging with FIDs, one can acquire a set of data without applied magnetic field gradients and use the above method (Figs. 3e and 3f) to obtain s_o. Then s_o can be included in the data sets, and the matrix suitably expanded. This constrains the area of the projections and sometimes makes other improvements (Fig. 4). An important benefit is that the condition number of the matrix can be lowered substantially, and one can get away with data sets that are not substantially oversampled.

Another method of reducing the condition number is to lie about q (Fig. 4). Within reason (about 10%), telling a computer that q is smaller than $T_d/\Delta t$ has an edge-enhancing effect on the projection, but does not destroy it. This will, of course, distort quantitative information obtained from the pixel values of an image.

ACKNOWLEDGMENTS

Thanks to Eiichi Fukushima and Steve Altobelli for paying attention to expostulations while we were formulating our ideas and for making very helpful comments. Thanks to Don Williams, Elaina Simplaceau, Maryann Butowicz, and Donald Bennett at PNMRCBR for helping D.O.K. during his visits to Pittsburgh. This work was supported by the NIH under Grants 1R29HL57967-01 to D.O.K. at LRRI and RR03631-04 to the PNMRCBR.

REFERENCES

1. H. Barkhuijsen, R. de Beer, and D. van Ormondt, Improved algorithm for noniterative time-domain model fitting to exponentially damped magnetic resonance signals, *J. Magn. Reson.* **73,** 553–557 (1987).
2. E. Fukushima and S. B. W. Roeder, "Experimental Pulse NMR: A Nuts and Bolts Approach," pp. 92–97, Addison–Wesley, Reading, MA (1981).
3. K. W. Vollmers, I. J. Lowe, and M. Punkkinen, A method of measuring the initial behavior of the free induction decay, *J. Magn. Reson.* **30,** 33–50 (1987).
4. R. W. Gerchberg, Super-resolution through error energy reduction, *Optica Acta* **21,** 709–720 (1974).
5. A. Papoulis, A new algorithm in spectral analysis and band-limited extrapolation, *IEEE Trans. Circuits Systems* **CAS-22,** 735–742 (1975).
6. A. Jain and S. Ranganath, Extrapolation algorithms for discrete signals with application in spectral estimation, *IEEE Trans. Acoust. Speech Signal Processing* **ASSP-29,** 830–845 (1981).
7. S. K. Plevritis and A. Macovski, Spectral extrapolation of spatially bounded images, *IEEE Trans. Med. Imag.* **14,** 487–497 (1995).
8. Z. P. Liang, F. E. Boada, R. T. Constable, E. M. Haacke, P. C.

Lauterbur, and M. R. Smith, Constrained reconstruction methods in MR imaging, *Rev. Magn. Reson. Med.* **4,** 66–185 (1992).

9. G. McGibney, M. R. Smith, S. T. Nicholas, and A. Crawley, Quantitative evaluation of several partial-Fourier reconstruction algorithms used in MRI, *Magn. Reson. Med.* **30,** 51–59 (1993).

10. D. O. Kuethe, A. Caprihan, E. Fukushima, and R. A. Waggoner, Imaging lungs using inert fluorinated gases, *Magn. Reson. Med.* **39,** 85–88 (1998).

11. D. P. Madio, H. M. Gach, and I. J. Lowe, Ultra-fast velocity imaging in stenotically produced turbulent jets using RUFIS, *Magn. Reson. Med.* **39,** 574–580 (1998).

12. P. T. Callaghan, "Principles of Nuclear Magnetic Resonance Microscopy," p. 13, Clarendon Press, Oxford (1991).

13. W. H. Press, B. P. Flannery, S. A. Teukolsky, and W. T. Vetterling, "Numerical Recipes in C: The Art of Scientific Computing," pp. 60–71, Cambridge Univ. Press, New York (1988).

14. C. L. Lawson and R. J. Hanson, "Solving Least Squares Problems," p. 123, Prentice Hall, Englewood Cliffs, NJ (1974).